Efficiency of Acetylcholine Receptor Subunit Assembly and Its Regulation by cAMP

Anthony F. Ross, William N. Green, Deborah S. Hartman, and Toni Claudio

Department of Cellular and Molecular Physiology, Yale University School of Medicine, New Haven, Connecticut 06510

Abstract. Assembly of nicotinic acetylcholine receptor (AChR) subunits was investigated using mouse fibroblast cell lines stably expressing either *Torpedo* (All-11) or mouse (AM-4) α, β, γ, and δ AChR subunits. Both cell lines produce fully functional cell surface AChRs. We find that two independent treatments, lower temperature and increased intracellular cAMP can increase AChR expression by increasing the efficiency of subunit assembly. Previously, we showed that the rate of degradation of individual subunits was decreased as the temperature was lowered and that *Torpedo* AChR expression was acutely temperature sensitive, requiring temperatures lower than 37°C. We find that *Torpedo* AChR assembly efficiency increases 56-fold as the temperature is decreased from 37 to 20°C. To determine how much of this is a temperature effect on degradation, mouse AChR assembly efficiencies were determined and found to be only approximately fourfold more efficient at 20 than at 37°C.

With reduced temperatures, we can achieve assembly efficiencies of *Torpedo* AChR in fibroblasts of 20–35%. Mouse AChR in muscle cells is also ~30% and we obtain ~30% assembly efficiency of mouse AChR in fibroblasts (with reduced temperatures, this value approaches 100%). Forskolin, an agent which increases intracellular cAMP levels, increased subunit assembly efficiencies twofold with a corresponding increase in cell surface AChR. Pulse–chase experiments and immunofluorescence microscopy indicate that oligomer assembly occurs in the ER and that AChR oligomers remain in the ER until released to the cell surface. Once released, AChRs move rapidly through the Golgi membrane to the plasma membrane. Forskolin does not alter the intracellular distribution of AChR. Our results indicate that cell surface expression of AChR can be regulated at the level of subunit assembly and suggest a mechanism for the cAMP-induced increase in AChR expression.

THE nicotinic acetylcholine receptor (AChR)[1] is a pentameric glycoprotein complex with the stoichiometry $\alpha_2\beta\gamma\delta$ which is localized to the postsynaptic surface of cholinergic synapses (for reviews see Popot and Changeux, 1984; Salpeter, 1987; Claudio, 1989). Although cell surface AChR expression is known to be regulated by signals from the innervating nerve terminal, the identity of these signals as well as the mechanisms by which AChR expression is regulated are not fully understood. Evidence exists for regulation at the level of mRNA transcription by neural factors (Harris et al., 1988; Horovitz et al., 1989), by muscle activity (Klarsfeld and Changeux, 1985; Goldman et al., 1988), by denervation (Goldman et al., 1985; Shieh et al., 1987; Tsay and Schmidt, 1989), and by the neuropeptide calcitonin gene-related peptide, (CGRP; Fontaine et al., 1987), which induces increased cAMP levels and which has been shown to be present in presynaptic terminals of the neuromuscular junction (Takami et al., 1985). However, in none of these studies do increases in subunit mRNA levels correlate tightly with changes in AChR cell surface expression, suggesting that there are additional sites of regulation of AChR expression.

One such site of regulation which might be especially important for a heterologous multisubunit protein complex, is subunit assembly. Assembly could be regulated by subunit availability or posttranslational modifications. If the addition of one subunit to the complex is rate limiting, then its expression, stability, or modifications to it could all be sites of regulation for assembly. Consistent with this, we have observed that the *Torpedo* β subunit has a much shorter half-life than the remaining three subunits (Claudio et al., 1989a), suggesting a possible regulatory role for this subunit. Regulation at the level of posttranslational modifications will be investigated in this article. We have shown previously that agents which increase intracellular levels of cAMP cause an increase in the number of cell surface AChRs expressed either in muscle cells or in fibroblasts (Green et al., 1991). The effect of one of these agents, forskolin, on subunit assembly and on the intracellular distribution of AChR will be described.

We also show that the efficiency of subunit assembly can be regulated by temperature. Assembly of *Torpedo* AChR is

---

1. *Abbreviations used in this paper*: AChR, acetylcholine receptor; BiP, binding protein; BuTx, Bungarotoxin; CGRP, calcitonin gene-related peptide; WGA, wheat germ agglutinin.

acutely temperature sensitive, occurring only at temperatures lower than 37°C (Paulson and Claudio, 1990). Although temperature would not be a mechanism for regulating assembly in vivo, we show that it is a method for improving assembly efficiencies for both temperature-sensitive proteins (such as the *Torpedo* proteins; Claudio et al., 1987) and nontemperature-sensitive proteins (such as mouse AChR) expressed in cultured mammalian cell lines. Thus, we can regulate the expression of an oligomeric protein at the level of subunit assembly by artificial methods (temperature) or by methods which appear to be working in vivo (altering the intracellular levels of cAMP).

Materials and Methods

Cell Lines

Cell lines were grown at 37°C in the presence of 5% CO_2 in DME supplemented with 10% calf serum. All-11 cells were prepared as described (Claudio et al., 1987). Briefly, these are mouse fibroblast L cells stably expressing all four *Torpedo californica* AChR subunits. Each subunit cDNA was engineered behind a SV-40 promoter (pSV2 vectors) and cotransfected with thymidine kinase into Ltk⁻ cells. Colonies were selected and grown in 15 μg/ml hypoxanthine, 1 μg/ml aminopterin, and 5 μg/ml thymidine (HAT). AM-4 cells are a stable cell line of mouse fibroblast NIH3T3 cells which have been cotransfected with the neomycin resistance gene (pSV2-neo) and the four mouse muscle (BC₃H-1) AChR subunit cDNAs engineered into pSV2 vectors. Colonies were selected in media containing 0.6 mg/ml G418 (Gibco Laboratories, Grand Island, NY). The AM-4 cell line expresses ∼0.5 picomole of cell surface AChRs per 35-mm dish (Sine, S.M., and T. Claudio, manuscript submitted for publication). To induce expression of *Torpedo* AChRs (All-11 cells), cells are grown at 37°C until confluent, 20 mM sodium butyrate is added for 24–36 h, and then the cells are placed in an incubator maintained at 20°C. To induce expression of mouse AChRs (AM-4 cells), cells are grown at 37°C until confluent, then 10 mM sodium butyrate is added for 24–36 h.

Labeling and Immunoprecipitations

Confluent 10-cm dishes of cells were washed twice with PBS, incubated for 15 min at 37°C with methionine-free media (JR Scientific, Woodland, CA), washed once with PBS, and then incubated with 2 ml methionine-free media containing 300 μCi [^{35}S]methionine (TRANS^{35}S; ICN Radiochemicals, Irvine, CA) for the given time and temperature in an atmosphere of 5% CO_2. Plates were rinsed three times with DME, 10 ml of chase media (DME, 10% calf serum, HAT, 20 mM sodium butyrate) were added and cells returned to the proper incubator. The remaining steps were carried out at 4°C. Cells were rinsed twice with PBS, scraped, and the cells pelleted by centrifugation at 5,000 g for 3 min. The pellets were resuspended in 300–500 μl of lysis buffer (150 mM NaCl, 5 mM EDTA, 50 mM Tris, pH 7.4, 1% Triton X-100, 0.02% NaN₃) containing fresh 2 mM PMSF and 2 mM N-ethylmaleimide, extracted 20 min, and the extracts clarified by centrifugation at 10,000 g for 10 min. Rabbit polyclonal antiserum directed against SDS gel-purified *Torpedo* AChR subunits (anti-α, -β, -γ, or -δ; Claudio and Raftery, 1977) or mAb 35 (American Type Culture Collection, Rockville, MD), an antibody specific to the α subunit, was added to supernatants and the samples were rocked overnight. 50 μl of protein A-Sepharose (diluted 2× in lysis buffer) was added, the samples were rocked a minimum of 3 h, and the resin washed five times with lysis buffer. After the final wash, 40 μl of gel-loading buffer (4% SDS, 20% glycerol, 0.125 M Tris, pH 6.8, 0.01% bromphenol blue) containing fresh 10 mM DTT was added to the pellets. The resins were removed by centrifugation and the supernatants were loaded onto either a 7.5 or 10% discontinuous SDS-polyacrylamide gel (Laemmli, 1970). Gels were fixed and stained for 30 min in 25% methanol and 10% acetic acid containing 0.5% Coomassie brilliant blue, destained, and then soaked in Amplify (Amersham Corp., Arlington Heights, IL) for 30 min, dried on a gel dryer, and exposed to film (X-Omat AR; Eastman Kodak Co., Rochester, NY) at −70°C with an intensifying screen. Densitometry was performed on a Unix scanner.

Endoglycosidase H and Endoglycosidase F Digestions

AChR subunits were labeled with [^{35}S]methionine and isolated by immu-

noprecipitation as described above. The subunits were dissociated from the protein A-Sepharose pellets in either 0.1 M sodium acetate, pH 5.5 (for endoglycosidase H treatment), or 0.1 M sodium phosphate buffer, pH 7.2 (for endoglycosidase F treatment), containing 0.5% SDS. The resin was removed by centrifugation, the supernatants were adjusted to 0.1% SDS in the appropriate buffer, and Triton X-100 was added to a final concentration of 0.5%. The subunits were then digested with either 3× 10⁻³ U of endoglycosidase H (Miles Scientific Division, Naperville, IL) or 20× 10⁻³ U of endoglycosidase F (Calbiochem-Behring Corp., San Diego, CA) overnight at room temperature. Samples were diluted 10-fold in lysis buffer, the δ subunit was re-immunoprecipitated with 2 μl of anti-δ subunit antiserum, and the immunoprecipitates were analyzed by SDS-PAGE.

Immunocytochemistry

Fibroblasts were grown on no. 1 glass coverslips until 75% confluent, incubated in 20 mM sodium butyrate for 24 h at 37°C, and then shifted to 20°C for 36 h. Cells were washed with PBS containing 0.005% CaCl₂ and 0.005% MgCl₂ (PBS/Ca/Mg), and fixed with 4% paraformaldehyde, 0.1% gluteraldehyde in PBS for 10 min at room temperature. They were then washed three times with PBS/Ca/Mg, and permeabilized using rapid dehydration and rehydration in ethanol. Nonspecific binding was blocked by incubating cells for 10 min in PBS/Ca/Mg containing 1.0% BSA. Cells were next labeled with mAbs which recognized assembled α subunits (a 1:30 dilution of mAb 35 or a 1:21 dilution of mAb 14; Tzartos and Lindstrom, 1980) or a 1:8 dilution of an mAb directed against heavy chain–binding protein (BiP; Bole et al., 1986) for 2 h at room temperature, then washed three times 10 min with PBS/Ca/Mg containing 0.1% BSA. Phycoerythrin-conjugated anti-rat IgG secondary antibody (Calbiochem-Behring Corp.) was diluted 1:40 in 0.1 M sodium phosphate, pH 7.0, containing 5 mg/ml BSA. Cells were incubated in secondary antibody for 1 h at room temperature, washed as above, and incubated in 20 μg/ml fluorescein-conjugated wheat germ agglutinin (WGA) for 10 min at room temperature. Cells were washed two times 5 min with PBS/Ca/Mg and rinsed briefly in distilled water before mounting in FluorSave (Calbiochem-Behring Corp.) on glass slides. Immunofluorescence was visualized in a microscope (model IM35; Zeiss, Oberkochen, Germany) equipped for fluorescence using a Nikon 60× objective with a numerical aperture of 1.4. Phycoerythrin fluorescence was detected using a rhodamine filter set (Zeiss). Cells were photographed directly on 400 ASA black and white film (Tri-X pan; Eastman Kodak Co., Rochester, NY) with exposure times of 15–20 s.

[^{125}I] α-Bungarotoxin (BuTx) Binding and Gradient Centrifugation

To measure cell surface AChR, All-11 cells were rinsed with PBS and incubated at room temperature in PBS containing 10 nM [^{125}I]BuTx (sp act 140–170 cpm/fmol; ICN Radiochemicals) and 0.1% BSA. Cultures were labeled for 2.5 h on a shaker table, washed three times with PBS, solubilized in lysis buffer containing 1% Triton X-100, and the radioactivity determined by γ-counting. Nonspecific binding, determined by measuring [^{125}I]BuTx binding in the presence of the competitive inhibitor carbamylcholine (1 mM), did not exceed 5% of total labeling. Total cellular AChR levels were determined by incubating cell lysates in 10 nM [^{125}I]BuTx for 3 h at 4°C on a rotator, followed by immunoprecipitation and γ-counting. For gradient fractionation, cell extracts were layered onto a 5.0 ml 5–20% linear sucrose gradient prepared in lysis buffer. Gradients were centrifuged in a rotor (model SW 50.1; Beckman Instruments, Palo Alto, CA) at 40,000 rpm to $\omega^2 t = 1.0 \times 10^{12}$. 15 fractions (330 μl) were collected from the top of the gradient, immunoprecipitated and analyzed as described.

Results

Temperature-dependent Assembly of Torpedo AChR Subunits

In a previous study, we determined that although *Torpedo* AChR subunit mRNA and polypeptides are produced at 37°C in AChR-fibroblasts, AChR complexes are not produced either internally or on the cell surface (Claudio et al., 1987). In another study, we established a cell line in which the *Torpedo* α subunit was stably expressed in rat L6 muscle cells. If the temperature was maintained at 37°C, only rat
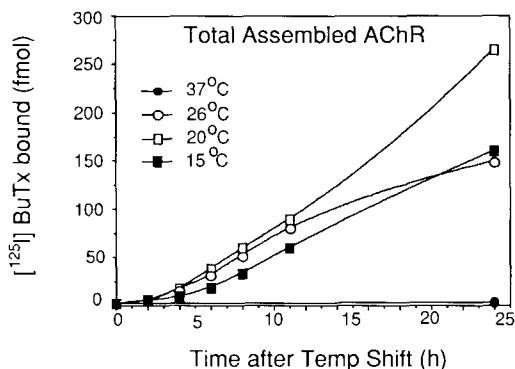
Figure 1. Temperature-dependent expression of *Torpedo* AChR oligomers. Confluent 10-cm plates of All-11 cells were incubated in 20 mM sodium butyrate in growth media for 24 h at 37°C and then shifted to 37, 26, 20, or 15°C for the indicated times in growth media containing 20 mM sodium butyrate. To measure total assembled AChR, cells were lysed and the cell lysates were incubated with 10 nM [^{125}I]BuTx for 3 h and then immunoprecipitated with polyclonal antisera specific for the δ subunit as described in Materials and Methods. (●) 37°C; (o) 26°C; (□) 20°C; (■) 15°C.

AChRs were formed. If the temperature was lowered, hybrid AChRs (containing either one or two *Torpedo* α subunits and the remainder endogenous rat subunits) were formed in addition to All-rat AChRs. The percentage of hybrids formed increased as the temperature was lowered, reaching $\sim$60% at the lowest temperature tested, 24°C (Paulson and Claudio, 1990). The defect in assembly appeared to be in the folding of the polypeptide chains.

To further investigate the temperature-sensitive phenomenon and determine if assembly efficiency is altered with temperature, we first determined the levels of assembled AChR expression at different temperatures. To induce AChR expression in the All-11 cells (*Torpedo* AChR-fibroblasts), confluent dishes of cells were placed in media containing sodium butyrate for 24 h at 37°C and then shifted to 15, 20, 26°C or left at 37°C. The levels of assembled AChR were measured by labeling extracts of All-11 cells with [^{125}I]BuTx followed by immunoprecipitation with antisera specific to the δ subunit. Since BuTx binds only to α subunits, immunoprecipitation with a non-α subunit-specific antiserum will measure only assembled AChR complexes. As shown in Fig. 1, no AChR is produced at 37°C; at 26°C, 149 fmole of AChR are expressed per 10-cm dish; and at 20°C, 264 fmole of AChR are produced. Because subunit synthesis rates are temperature dependent and the assay used measures predominantly newly synthesized AChR, it would be expected that AChR levels would decrease with decreasing temperature. The observation that the amount of assembled AChR decreases from 20 (264 fmole) to 15°C (159 fmole) probably reflects such a temperature-dependent synthesis rate. Our result that assembled AChR levels actually increase when going from 37 to 20°C indicates a temperature effect on something other than rate of synthesis. Two processes were investigated for temperature dependency, assembly and rate of AChR degradation.

To measure subunit assembly efficiency, it is necessary to distinguish unassembled from assembled subunits. This is most clearly done by following the migration of subunits on sucrose gradients. Unassembled subunits migrate as broad

peaks centering around 6S whereas AChR pentamers form sharp peaks centering at 9S (Paulson, H. P., A. F. Ross, W. N. Green, and T. Claudio. In press.). Another method of assaying for assembly is by the coimmunoprecipitation of three subunits with antibodies directed against the fourth subunit. A third method is with conformation-specific mAbs. One of the conformation-specific mAbs used in this study is mAb 35, an antibody directed against the α subunit (Tzartos and Lindstom, 1980). Although this mAb will bind unassembled α subunits, it binds preferentially to α subunits which are part of an $\alpha_2\beta\gamma\delta$ pentamer. mAb 35 will precipitate 85–90% of [^{125}I]BuTx labeled surface AChR in All-11 cells (data not shown) but only 5.5% of unassembled α in these cells (determined by comparing the amount of α immunoprecipitated by mAb 35 in Fig. 2 *B* with α immunoprecipitated by polyclonal anti-α antisera in *A*, see below). All three methods were used to measure assembly efficiency as a function of temperature.

Cells were pulse labeled at 37°C for 30 min with [^{35}S] methionine, lysed immediately or after a given chase period, and the cell lysates separated on a 5–20% linear sucrose gradient. Fractions were then immunoprecipitated with either a cocktail of polyclonal antibodies directed against each of the four subunits (to determine total polypeptide synthesis) or with mAb 35 (to determine assembled AChR complex). Immunoprecipitates were analyzed by SDS-PAGE autoradiography (Fig. 2, *left panels*), the bands were scanned, and plotted against the gradient fraction number (Fig. 2, *right panels*).

After such a pulse–chase protocol, we measured the assembly of each of the four subunits. As shown in Fig. 2 *A*, the labeled subunits isolated immediately after the pulse (unassembled) using a cocktail of subunit-specific antisera extend broadly (fractions 6–12) across the gradient. Assembled AChR (noted with an arrow) runs as a sharp peak in fraction 9 (Fig. 2 *D*). When a parallel lysate was immunoprecipitated with mAb 35, the α subunit alone was immunoprecipitated and it too, was distributed across the gradient in a broad fashion (Fig. 2 *B*). When cells were chased for increasing lengths of time at 20°C, however, there was a gradually increasing coprecipitation of the β, γ, and δ subunits in the 9S peak (Fig. 2, *C* and *D*), as well as a shift of the α subunit from a broad 6S–13S profile into a sharp 9S peak (Fig. 2 *D*). This 9S peak comigrates precisely with cell surface AChR labeled with [^{125}I]BuTx (Fig. 2, *arrow*), showing that this internal population represents fully assembled AChR oligomers. We can measure the efficiency of assembly by calculating the percentage of subunits labeled during the pulse which can be chased into the assembled population.

To determine the effect of different temperatures on the time course and efficiency of subunit assembly, cultures were pulse labeled at 37°C and chased at 37, 26, or 20°C for 0–72 h. After lysis, the cell extracts were immunoprecipitated with mAb 35 and the amounts of coprecipitated β, γ, and δ subunits were measured by densitometry (Fig. 3). The most striking result is the increased coprecipitation of subunits at 20 compared to 26°C, showing that assembly is significantly more efficient at 20°C. The peak of assembly at 26°C occurred at $\sim$12 h of chase, with total assembled AChR decreasing thereafter, probably because of degradation of assembled AChR. At 20°C, however, peak levels of assembly occurred at $\sim$30 h of chase, and total assembled
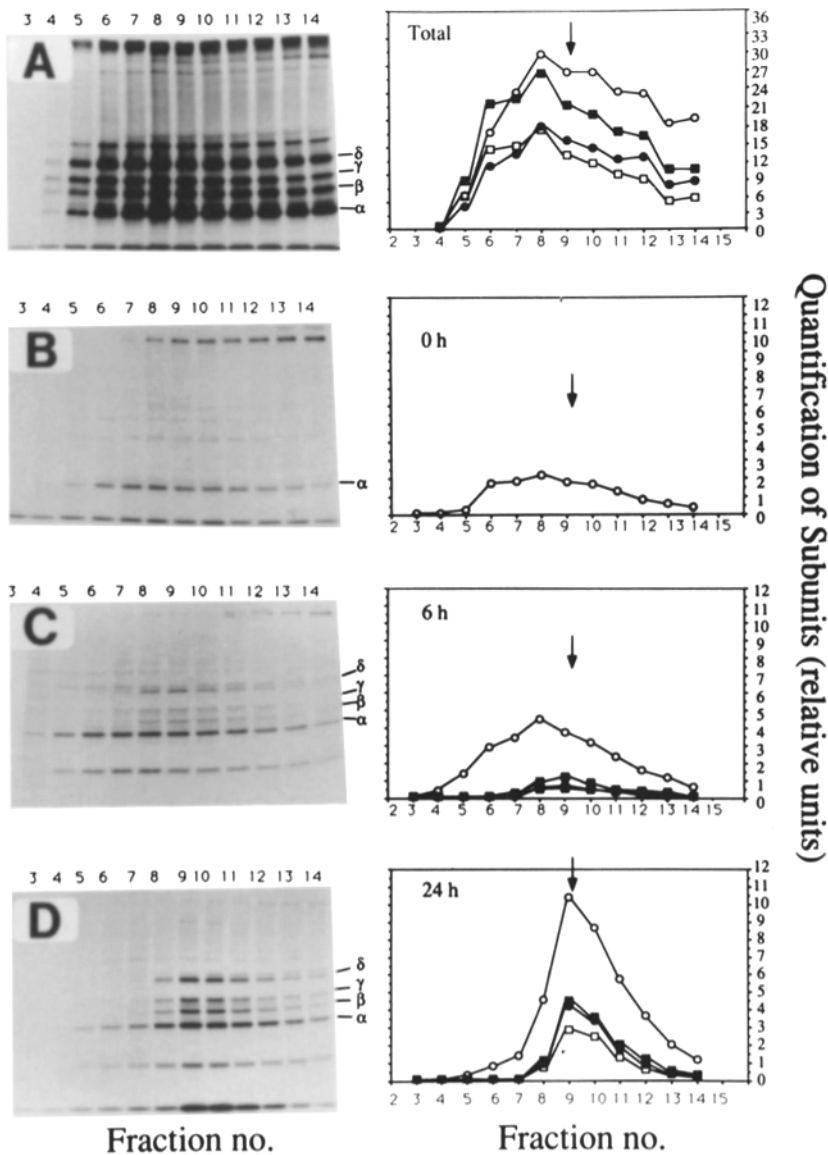
Figure 2. Assembly of *Torpedo* AChR subunits monitored by sucrose gradient centrifugation. Confluent 10-cm plates of All-11 cells were pulse labeled for 30 min with 150 μCi/ml [^{35}S]-methionine, rinsed three times with DME, and either lysed immediately or chased at 20°C in growth media for 6 or 24 h before lysis. Cell lysates (two plates per condition) were labeled with 10 nM [^{125}I]BuTx for 3 h at 4°C, layered on a 5-20% linear sucrose gradient and run at 100,000 g to $\omega^2 t = 1.0 \times 10^{12}$. 15 fractions (330 μl each) were collected from each gradient and immunoprecipitated with either a cocktail of polyclonal antisera (*A*) or with mAb 35 (*B*, 0-h chase; *C*, 6-h chase; *D*, 24-h chase). Immunoprecipitated material was analyzed by SDS-PAGE on 7.5% gels (left side) and the subunit bands quantified by densitometry (right side). (O) α subunit; ($\bullet$) β subunit; ($\square$) γ subunit; ($\blacksquare$) δ subunit. The arrow marks the position of migration of the AChR pentamer in each gradient which was determined by running a parallel gradient of [^{125}I]BuTx-labeled cell surface AChR (not shown).

AChR decreased only slightly over the remainder of the chase period. The assembly efficiencies of all four subunits as a function of temperature are given in Table I. As shown, the assembly efficiencies were ~0.4% at 37°C, ~2.5% at 26°C, and ~22.4% at 20°C. These values are averages of the efficiency of assembly of the β, γ, and δ subunits at each temperature. The values obtained for α at each temperature are a little higher because they reflect assembled plus some unassembled subunit since an anti-α subunit antibody was used for the immunoprecipitation (discussed above).

Interestingly, the pulse temperature did not affect the assembly efficiency. For example, the efficiencies of assembly of β, γ, δ at 26°C averaged 2.6% when pulsed at 26°C and 2.4% when pulsed at 37°C. Similarly, assembly efficiencies of β, γ, δ at 20°C averaged 24.4% when pulsed at 20°C and 21.5% when pulsed at 37°C. Thus, although subunits synthesized at 37°C cannot assemble at 37°C, once the temperature is lowered to a permissive temperature, assembly occurs as efficiently as when the subunits are synthesized at the permissive temperature. In a previous study of the temperature-

sensitive phenomenon, we determined (using two independent measures of polypeptide conformation) that the defect in assembly at 37°C was because of misfolded polypeptides (Paulson and Claudio, 1990). The observation that polypeptides synthesized at 37°C assemble as efficiently as subunits synthesized at the permissive temperatures demonstrates that the assembled subunits were not irreversibly misfolded.

Assembly of Mouse AChR Subunits at Different Temperatures

Part of the observed increase in assembly efficiency with decreasing temperature could be explained by a decrease in the rate of protein degradation. In All-11 cells, there is an approximate fourfold increase in half-life of unassembled subunits as the temperature is decreased from 37 to 26°C (40 min to 3 h, respectively) and an approximate fourfold increase as the temperature is decreased from 26 to 20°C (3 h to 14 h, respectively). To determine if changes in temperature can affect the assembly efficiency of an AChR which normally assembles at 37°C, we used our NIH3T3 cell line
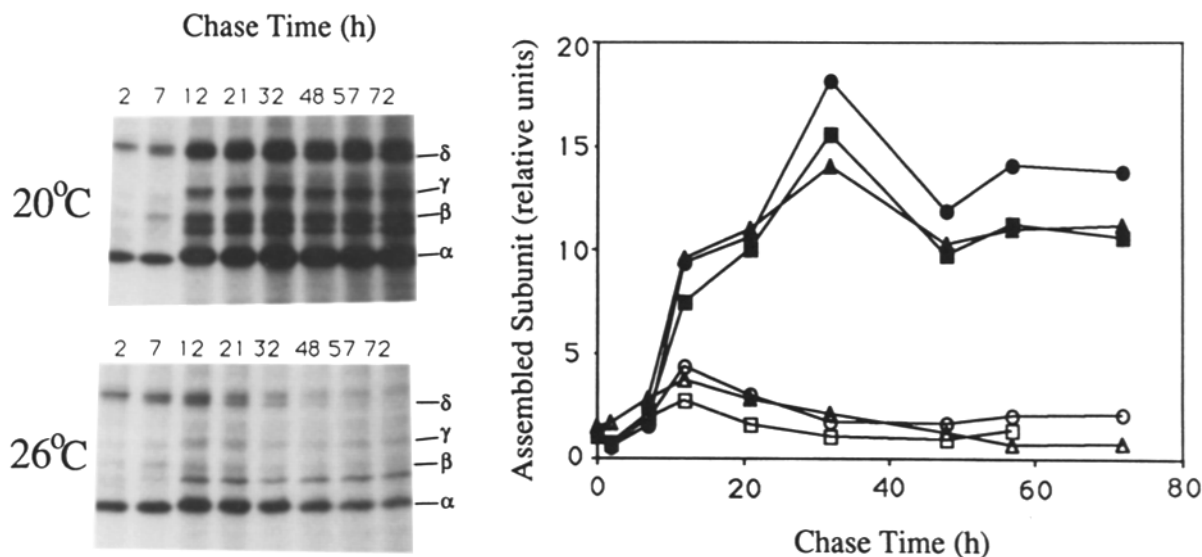
Figure 3. Temperature-dependent assembly of *Torpedo* AChR subunits. Confluent 10-cm plates of All-11 cells were incubated in growth media containing 20 mM sodium butyrate for 24 h at 37°C, then pulse labeled for 30 min with 150 μCi/ml [^{35}S]methionine at 37°C, rinsed three times with DME, and chased at either 20 or 26°C in growth media with 20 mM sodium butyrate. At the indicated times, plates were lysed and immunoprecipitated with mAb 35. The immunoprecipitates were analyzed by SDS-PAGE on 7.5% gels (left) and the β, γ, and δ subunit bands quantified by densitometry (right). ($\bullet$, $\blacksquare$, $\blacktriangle$) 20°C chase; (o, $\square$, $\triangle$) 26°C chase. ($\square$, $\blacksquare$) β subunit; ($\triangle$, $\blacktriangle$) γ subunit; (o, $\bullet$) δ subunit.

which stably expresses all four mouse AChR subunits (AM-4 cells). These cells express high levels of cell surface AChR which have electrophysiological and pharmacological properties similar to AChR in mouse BC$_3$H-1 muscle cells (Sine, S. M., and T. Claudio, manuscript submitted for publication). AM-4 cells were pulse labeled with [^{35}S]methionine for 10 min at 37°C, chased for various times, and assembly was monitored as before (coimmunoprecipitation of subunits with subunit-specific mAbs or shifts into the assembled pool monitored by sucrose gradient sedimentation). Our polyclonal anti-*Torpedo* α subunit antisera, which cross reacts

with mouse α subunit (Fig. 4), was used to immunoprecipitate total mouse α subunit while mAb 35 was used to immunoprecipitate assembled mouse AChR. The identities of the four mouse AChR subunits were established either by Western blotting or by comparison to cell lines expressing specific combinations of subunits (established by cotransfecting just some of the subunit cDNAs).

Extracts from cells lysed immediately after the pulse were run on a sucrose gradient, the fractions were immunoprecipitated with anti-α antisera, and analyzed by SDS-PAGE autoradiography. As shown in Fig. 4 *A*, mouse α subunit was distributed across broad regions of the gradient, similar to that of *Torpedo* α in All-11 cells (Fig. 2 *B*). When cells were chased for 5 h at 37°C and immunoprecipitated with mAb 35, all four subunits were identified in the 9S peak (Fig. 4 *B*, fractions 10 and 11). Both intracellular and cell surface forms of the γ and δ subunit (see legend to Fig. 4) were seen, indicating that some of the pulse–labeled AChR was transported to the cell surface by this time of chase. To establish more fully the time-course of assembly and intracellular transport, cells were pulse labeled for 10 min, chased for various times, and the coimmunoprecipitation of the β, γ, and δ subunits with mAb 35 was monitored. As shown in Fig. 5, small amounts of the β, γ, and δ subunits were coimmunoprecipitated at the end of the pulse period and these amounts were seen to increase with increasing chase times. The cell surface form of the δ was clearly evident at 120 min of chase.

The time courses of assembly show that *Torpedo* AChRs assemble slower than mouse AChRs even at the same temperatures. Assembled mouse AChRs are first detected at $\sim$20 min after synthesis (10 min label plus 10 min chase) at 37°C, and $\sim$2 h at 20°C (see later discussion and Fig. 6). In contrast, intracellular assembly of *Torpedo* AChR in fibroblasts is first detected at $\sim$2 h at 26°C and $\sim$6 h at 20°C.

Table I. Temperature-dependent Assembly of Torpedo AChR Subunits

		°C			
Pulse	37	37	26	37	20
Chase	37	26	26	20	20
			%		
Subunit δ	0.5	3.3	1.6	22.9	23.6
γ	0.4	2.4	1.7	19.9	23.3
β	0.4	1.7	4.5	21.8	26.3
α	1.5	8.5	4.1	33.4	36.5

Confluent 10-cm plates of All-11 cells were incubated with 20 mM sodium butyrate in growth media for 24 h at 37°C, then pulse labeled with 300 μCi/ plate of [^{35}S]methionine for 30 min at the indicated temperature (Pulse Temp). Two plates from each condition were then harvested and all labeled subunits were isolated by immunoprecipitation with polyclonal antisera directed against *Torpedo* α, β, γ, and δ subunits. The remaining plates (two per condition) were rinsed and chased for 4 h (37°C chase), 24 h (26°C chase), or 30 h (20°C chase). Plates were rinsed, lysed, and assembled subunits were immunoprecipitated with mAb 35 as described in Materials and Methods. Subunits were separated by SDS-PAGE asnd quantified by autoradiography followed by densitometric scanning. The efficiency of assembly for each subunit was calculated by measuring the percentage of subunit initially present after the pulse which was chased into an assembled complex. Values are the mean of two determinations; SD did not exceed 10% of the total.
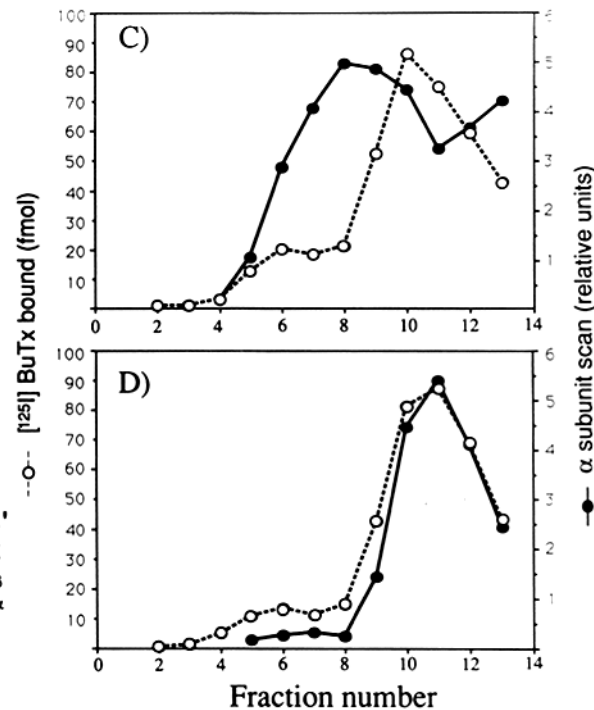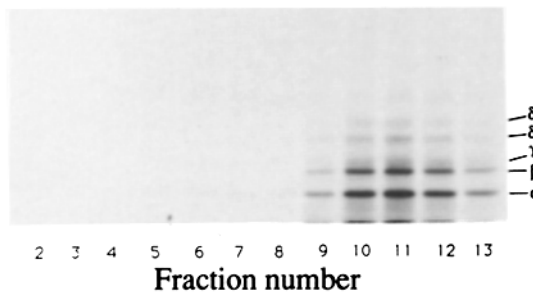
A) Total α subunit
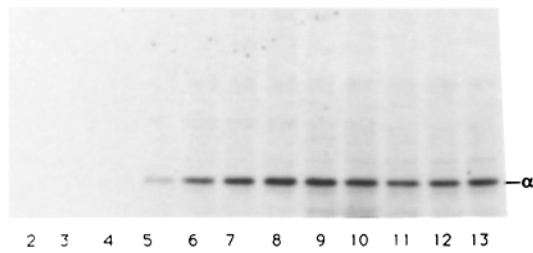
B) Assembled AChR

Figure 4. Assembly of mouse AChR monitored by sucrose gradient centrifugation. Confluent 10-cm plates of AM-4 cells (mouse AChR-fibroblasts) were incubated in growth media containing 10 mM sodium butyrate for 24 h at 37°C, then pulse labeled for 15 min with 150 μCi/ml [^{35}S]methionine. Cells were harvested either immediately (*A*) or after a 5-h chase at 37°C (*B*). Cell lysates were incubated with [^{125}I]BuTx for 3 h, then fractionated on a 5–20% sucrose density gradient at 40,000 rpm to $\omega^2 t = 1.0 \times 10^{12}$. Fractions were immunoprecipitated with either 2 μl of anti-*Torpedo* α subunit antiserum (*A*) or 15 μl of mAb 35 (*B*), and analyzed by SDS-PAGE autoradiography on 7.5% gels. The α subunit bands were quantified by densitometry and are plotted along with the immunoprecipitated [^{125}I]BuTx/AChR complexes at right. Note that newly synthesized α subunit exhibits a broad gradient profile (*solid line*), while assembled α subunit fractionates in a 9S peak which is identical to that of [^{125}I]BuTx/AChR complexes (*dotted line*). α, β, γ, and δ refer to the intracellular forms of the subunits and δ' refers to the cell surface form of the δ subunit. The apparent electrophoretic migrations of the subunits are 42, 48, 51, 61, and 64 kD for α, β, γ, δ, and δ' respectively. The shift in migration of the δ subunit from 61 kD (intracellular form) to 64 kD (cell surface form) is consistent with observations made in C2 muscle cells (Gu et al., 1989) where it is believed that the two mobilities reflect differences in the attached carbohydrates. A similar but smaller shift is seen with the γ subunit, which appears in these gels as a broad band from 51–53 kD (see also Fig. 5).

The efficiency of assembly of the mouse subunits was determined by measuring the percentage of α subunit labeled during the pulse which could be chased into an assembled 9S pool. At 37°C, maximum assembly was seen at ∿5 h of chase, with ∿30% of the pulse-labeled α subunit being assembled at this time (Fig. 4 *B*). This number agrees well with published data in which only ∿30% of the α subunit in BC₃H-1 muscle cells assembles (Merlie and Lindstrom, 1983). Thus, NIH3T3 fibroblasts can assemble muscle AChR as efficiently, and with a similar time course, as muscle cells. Because of a paucity of subunit-specific antibodies to muscle β, γ, and δ subunits and thus the difficulty of quantitatively immunoprecipitating them, we were unable to directly measure the assembly efficiency of these subunits. However, we measured the relative assembly efficiencies as a function of temperature by comparing the amounts coimmunoprecipitated with mAb 35 when cells were chased at 37, 26, or 20°C (Table II and Fig. 6). As shown, when cells were chased at 37°C, the amount of assembled subunit peaked at ∿5 h of chase and declined thereafter; at 26°C, assembled subunits peaked at 5–10 h of chase and remained constant thereafter; at 20°C, assembly continued to increase up to 30 h of chase.

Comparing the peak fractions, the assembly efficiency of all four subunits increased 1.7- to 2.9-fold at 26°C and 2.5- to 4.5-fold at 20°C (Table II). It is evident from these results, however, that at 37°C degradation of assembled AChRs is significant and sufficient to cause a loss of all detectable signal by 21 h of chase (Fig. 6, ●). At 26 and 20°C, it appears that degradation of assembled AChR oligomers is significantly reduced, which would result in the observed increase in assembly efficiency. For mouse AChR, assembly efficiency was increased ∿3.8-fold (average of the β, γ, and δ subunits) by reducing the temperature from 37 to 20°C. As determined in the previous section, *Torpedo* AChR assembly efficiency was increased 56-fold (average of β, γ, and δ) from 37 to 20°C. It is likely that only 3.8- of the 56-fold increase is because of decreased protein degradation. This would indicate then, that there was a ∿15-fold increase in *Torpedo* AChR assembly efficiency that was because of factors other than protein degradation: for example, polypeptide conformation, subunit–subunit interaction time.

In general, the amount of labeled, assembled AChR seen at any given time represents a balance between assembly and degradation. For mammalian AChR, the assembly efficien-
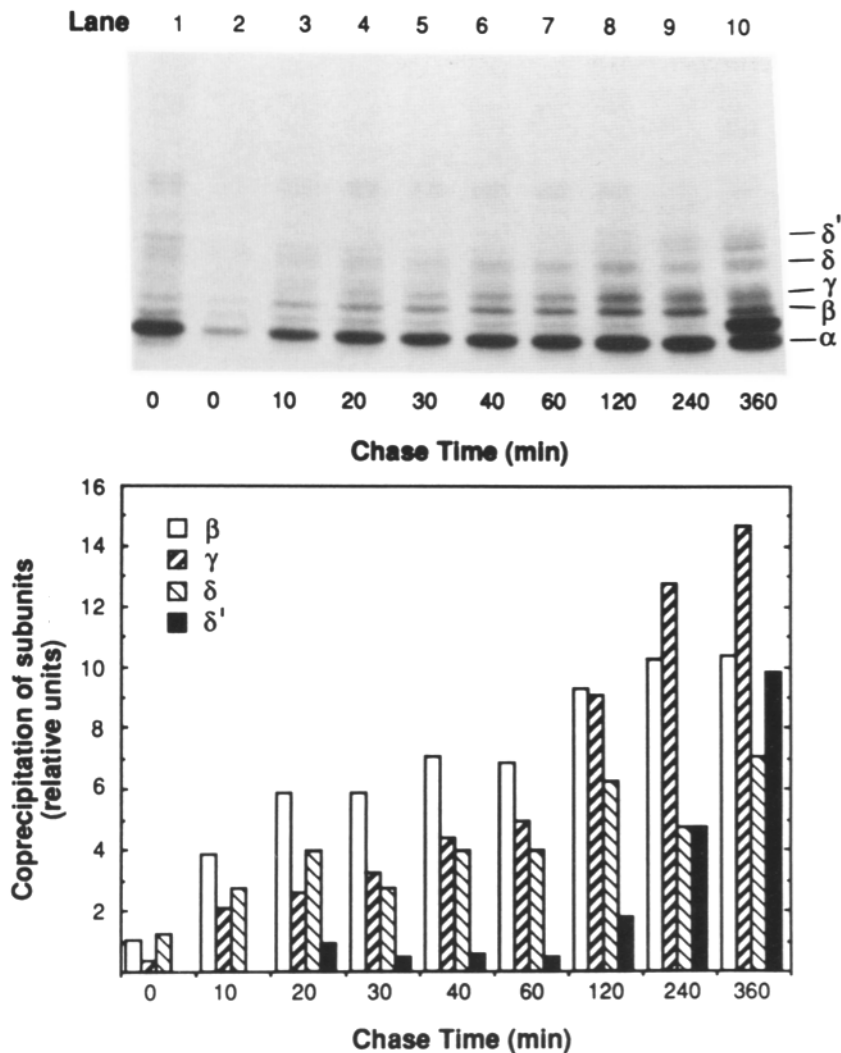
Figure 5. Time course of assembly of mouse AChR subunits. Confluent 10-cm plates of AM-4 cells were incubated in growth media containing 10 mM sodium butyrate for 24 h at 37°C, then pulse labeled for 10 min with 150 μCi/ml [³⁵S]methionine. Cells were harvested either immediately or after the given chase period. Cell lysates were immunoprecipitated with either 2 μl of anti-*Torpedo* α subunit antiserum (lane *1*) or 15 μl of mAb 35 (lanes *2-9*). Samples were analyzed by SDS-PAGE autoradiography on a 7.5% gel. The positions of the subunits are marked α, β, γ, δ and δ' (see legend to Fig. 4). The γ subunit appears initially as a distinct band at 51 kD which represents the intracellular form, and becomes broad as the surface form (53 kD) appears at ∿120 min of chase. The β, γ, δ, and δ' subunit bands were quantified by densitometry and are plotted in bottom panel.

cies are probably similar at all temperatures but practically, by reducing protein degradation with decreased temperatures, one can increase assembly and achieve higher levels of cell surface AChRs. For *Torpedo* and other temperature-sensitive protein complexes, reduced temperatures also greatly affect the ability of the subunits to assemble.

Effect of Forskolin on AChR Expression and Assembly Efficiency

We have previously reported that a variety of agents (forskolin, cholera toxin, theophyllin, and cAMP analogs) which increase intracellular cAMP levels induce marked increases in cell surface AChR levels in All-11 cells (Green et al., 1991). Forskolin, a widely used stimulator of adenylate cyclase activity, induced a two- to threefold increase in cell surface AChRs for both *Torpedo* AChRs expressed in AChR-fibroblasts and endogenous rat AChRs expressed in rat L6 muscle cells. For both systems, the forskolin effect was shown to be mediated through a posttranslational mechanism. Further analysis of the forskolin effect in AChR-fibroblasts demonstrated that the half-lives of the unassembled subunits each increased 1.9- to 2.8-fold. To test if forskolin

acts by influencing the subunit assembly process directly, All-11 cells were pulse labeled at 37°C, shifted to 20°C in the presence or absence of forskolin, and the efficiency of assembly was monitored. As shown in Fig. 7, when cells were pulse labeled at 37°C for 30 min, chased at 20°C for 6 h, and assembled AChR was isolated by immunoprecipitation, forskolin was found to induce a marked (two- to threefold) increase in the accumulation of all four subunits in the 9S peak. Since the cells were treated with forskolin after the pulse period, this result demonstrates that forskolin increases the conversion of subunits from the unassembled to the assembled state. Analysis of the time course of assembly in the presence of forskolin shows that at times ≥6 h, there is increased assembly which correlates with increased [¹²⁵I]BuTx binding (Fig. 8). These results suggest that forskolin mediates the increase in AChR expression by increasing subunit assembly efficiency.

It is possible that forskolin has effects at additional points along the AChR biosynthetic pathway, such as the release of assembled AChR from an intracellular compartment. To address this question, we first determined where in the cell AChR subunits assembled and then investigated the possible effects of forskolin on this localization.
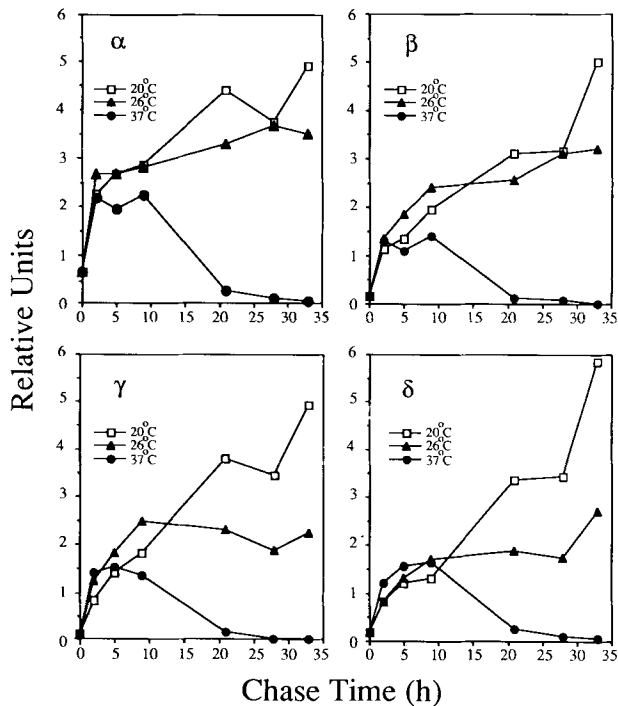
Figure 6. Effect of lower temperature on assembly of mouse AChR. 10-cm plates of AM-4 cells were incubated in growth media containing 10 mM sodium butyrate for 24 h at 37°C, then pulse labeled at 37°C for 15 min with 150 μCi/ml [³⁵S]methionine. One plate was havested immediately after the pulse (to determine total labeled subunit), the remaining plates were chased at either 37°C (●) 26°C (▲) or 20°C (□) for the indicated times. After each chase period, cells were lysed and immunoprecipitated with 15 μl of mAb 35. Samples were analyzed by SDS-PAGE autoradiography on a 7.5% gel, and the subunit bands quantified by densitometry. The ratio of each subunit band at the given chase time relative to the total amount of that subunit labeled at time 0 is plotted as Relative Units.

Localization of Intracellular AChR by Endoglycosidase H Sensitivity

To determine the intracellular location of assembled and unassembled AChR subunits in All-11 cells, we monitored the

Table II. Effect of Temperature on Assembly of Mouse AChR

		°C		
Pulse		37	37	37
Chase		37	26	20
Subunit	δ	1	1.7	3.7
	γ	1	1.5	3.3
	β	1	2.9	4.5
	α	1	1.8	2.5

Confluent 10-cm plates of AM-4 cells were incubated in media supplemented with 20 mM sodium buryate for 24 h at 37°C, then pulse labeled with 300 μCi/ plate of [³⁵S]methionine for 30 min at the given temperature. The plates were rinsed and chased for 5 h (37°C), 24 h (26°C), or 30 h (20°C). These chase times allowed the maximum amount of assembly to occur at the given temperature (see Fig. 6). Plates were rinsed, lysed, and assembled subunits immunoprecipitated with mAb 35 as described in Materials and Methods. Subunits were separated by SDS-PAGE and quantified by autoradiography followed by densitometry. The values given represent the ratio of the total amount of assembled subunit compared to that at 37°C.

sensitivity of the δ subunit isolated from these pools with endoglycosidase H. Simple asparagine-linked carbohydrate side chains are sensitive to this glycosidase, but when converted to the complex type by enzymes located in the medial Golgi apparatus, they become endoglycosidase H resistant (Roth, 1987). We have analyzed *Torpedo* AChR subunits expressed in fibroblast cell lines and determined that they contain one, one, two, and three units of asparagine-linked oligosaccharides for the α, β, γ, and δ subunits, respectively (Claudio et al., 1989a). Nomoto et al. (1986) analyzed the oligosaccharides obtained after digestion of each *Torpedo* subunit isolated from electroplax and obtained data that were consistent with such a pattern. They found that the α and β subunits contained only simple, high mannose-type carbohydrates while the γ and δ subunits contained both simple and complex carbohydrates.

Unassembled δ subunit, δ subunit from intracellular assembled AChR complexes, and δ subunit from cell surface AChRs were isolated according to the protocol given in the legend to Fig. 9 and digested with either endoglycosidase H or endoglycosidase F (both simple and complex carbohydrates are sensitive to this latter glycosidase) as described in Materials and Methods. Unassembled δ subunits were found to be digested completely by both endoglycosidase H and endoglycosidase F, showing that these subunits are not transported as far as the medial Golgi (Fig. 9, lanes *2* and *3*). Similarly, δ subunits isolated from intracellular assembled AChRs were completely cleaved by both enzymes, showing that this pool of AChR had not passed through the medial Golgi (Fig. 9, lanes *5*, *6*, *8* and *9*). Complete endoglycosidase H sensitivity was seen in the intracellular assembled δ subunit both in pulse–chase experiments (Fig. 9) and when the cells were labeled for 24 h with no chase (not shown), conditions in which the entire pool of δ subunit would be labeled. In contrast δ subunits isolated from cell surface AChR were completely cleaved by endoglycosidase F (Fig. 9, lanes *11* and *14*) but were partially resistant to endoglycosidase H (Fig. 9, lanes *12* and *15*), showing that these AChRs had passed through the medial Golgi and acquired complex oligosaccharides. Careful analysis of the endoglycosidase H pattern shows that the carbohydrates on the δ subunit are heterogeneous, as shown by the doublets in Fig. 9, lanes *12* and *15*. We can conclude from these data that (*a*) AChR subunits assemble before transport to the medial Golgi; (*b*) the majority of intracellular assembled AChRs reside in compartments before the medial Golgi at both 20 and 26°C and, (*c*) once complex carbohydrate moieties have been added in the medial Golgi apparatus, transport to the cell surface is rapid. The latter two conclusions are based on the observation that no intracellular AChRs were isolated which contained complex oligosaccharides.

Immunofluorescent Localization of Intracellular AChR

To further localize intracellular assembled and unassembled AChR, cells were examined by immunofluorescent microscopy. The results from the endoglycosidase H experiments demonstrated that AChRs assemble before the medial Golgi apparatus. Does assembly occur in the *cis*-Golgi, in a region between the ER and the Golgi apparatus, or in the ER? All-11 cells were grown at 37°C until confluent, incubated in so-
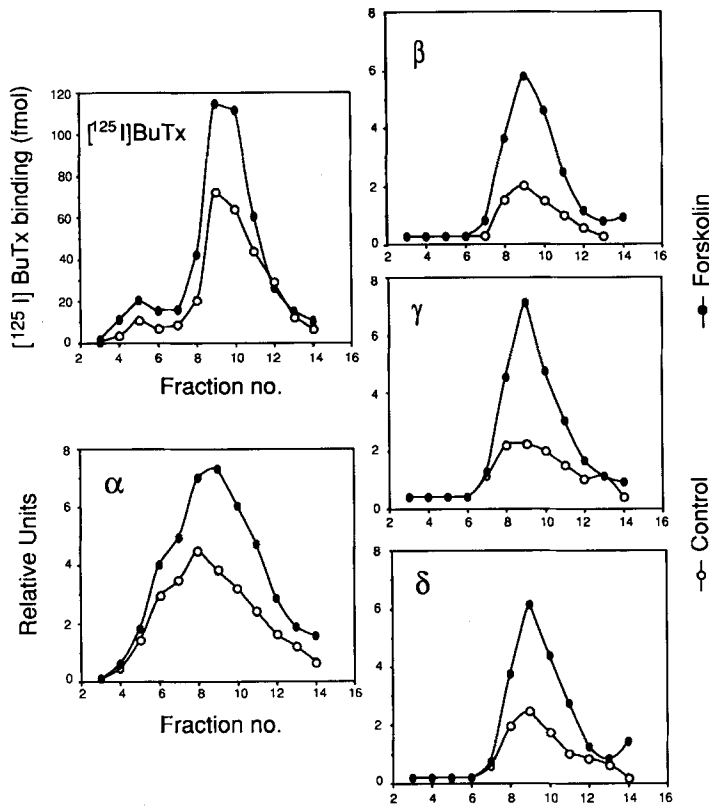
Figure 7. Effect of forskolin on assembly of *Torpedo* AChR subunits monitored by sucrose gradient centrifugation. All-11 cells were pulse labeled with 150 μCi/ml [^{35}S]methionine for 30 min at 37°C, shifted to 20°C in the presence or absence of 100 μM forskolin for 6 h, and the cells lysed. Cell lysates were incubated with 10 nM [^{125}I]BuTx for 3 h and fractionated on 5–20% linear sucrose gradients run at 100,000 g to $\omega^2 t = 1.0 \times 10^{12}$. Fractions were collected, immunoprecipitated with mAb 35, and counted in a γ-counter (upper left). Immunoprecipitates were then analyzed by SDS-PAGE autoradiography on 7.5% gels and the subunit bands in each fraction quantified by densitometry (remaining panels, marked α, β, γ, or δ). (O) control cells; (●) forskolin-treated cells. In the upper left panel ([^{125}I]BuTx-binding material), the small peak in fraction #5 (5S) is unassembled α subunit. In the remaining panels, in which subunits are quantified across the gradient, the peak for each [is al]so located in the 9S fraction.
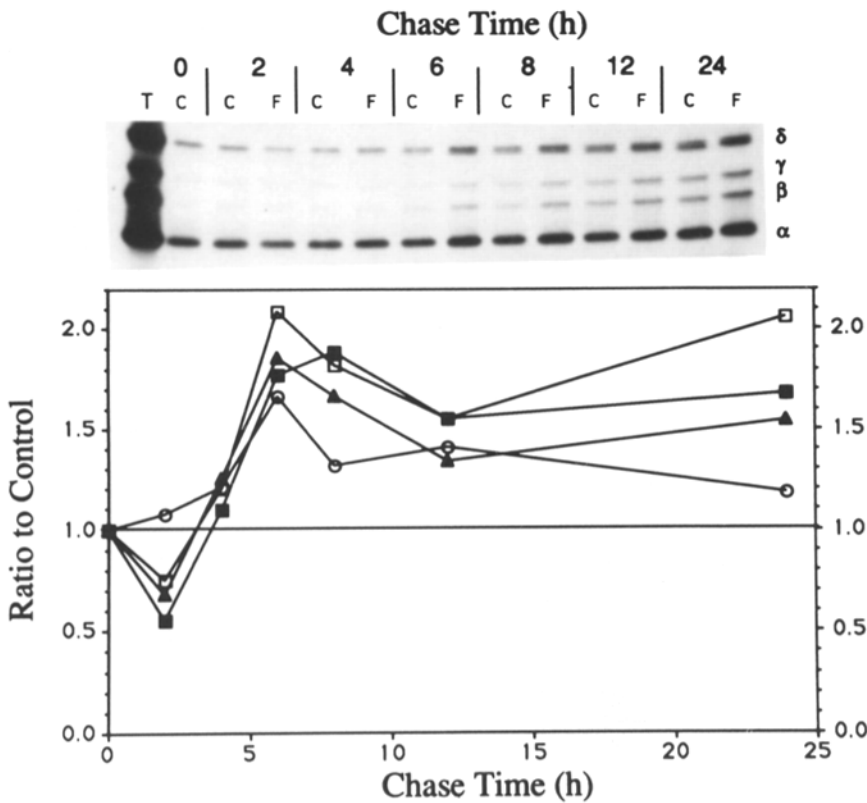

Figure 8. Effect of forskolin on the time course of assembly of *Torpedo* subunits. All-11 cells were pulse labeled with 150 μCi/ml [^{35}S]methionine for 15 min at 37°C, shifted to 20°C in the presence or absence of 100 μM forskolin for the given time, and then the cells were lysed. Cell lysates were incubated with 10 nM [^{125}I] BuTx for 3 h, the lysates immunoprecipitated with mAb 35, and the immunoprecipitates analyzed by SDS-PAGE autoradiography (top). The β, γ, and δ subunit bands were quantified by densitometry and are expressed in the lower panel as ratios of forskolin-treated cells to control cells. Top: (*C*) control cells; (*F*) forskolin-treated cells; (*T*) lysate immunoprecipitated with polyclonal antisera to α, β, γ, and δ subunits. Bottom: (O) [^{125}I]BuTx counts measured before SDS-PAGE; (□) β subunit; (■) γ subunit; (▲) δ subunit.
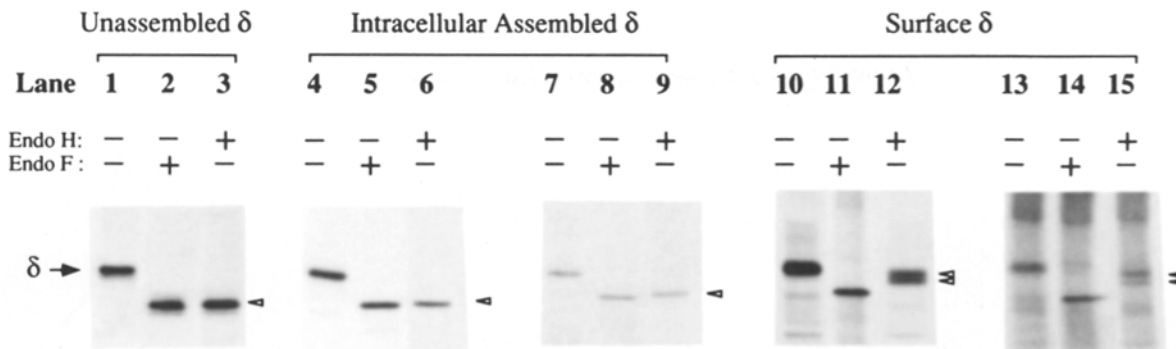
Figure 9. Endoglycosidase H sensitivity of cell surface, intracellular assembled, and unassembled δ subunit. Confluent 10-cm plates of All-11 cells were pulse labeled with 150 µCi/ml [³⁵S]methionine at 37°C for 30 min, chased for 24 h at either 20 or 26°C, and the surface AChRs, intracellular assembled AChRs, and intracellular unassembled δ subunits were isolated by sequential immunoprecipitation as follows. Cells were labeled with 10 nM [¹²⁵I]BuTx for 3 h at 4°C, rinsed five times with PBS and lysed. Cell surface AChR was immunoprecipitated with 2 µl of anti-BuTx antiserum (T. Claudio, unpublished results) followed by protein A-Sepharose. The lysates were then incubated with 15 µl of mAb 35 followed by protein A-Sepharose to immunoprecipitate intracellular assembled AChR. Unassembled δ subunit was isolated by lysing cells immediately after a 30-min pulse at 37°C and immunoprecipitating the lysates with anti-δ subunit antisera. The subunits were removed from the pellets and digested overnight at 25°C with endoglycosidases H or F as described in Materials and Methods. After digestion, the δ subunit was reimmunoprecipitated with anti-δ subunit antisera, and analyzed by SDS-PAGE autoradiography. Arrows mark the position of the δ subunit in untreated cells. (Lanes *1–3*) Unassembled δ; (lanes *4–6*) intracellular assembled δ isolated from cells chased at 20°C for 24 h; (lanes *7–9*) intracellular assembled δ isolated from cells chased at 26°C for 24 h; (lanes *10–12*) surface δ isolated from cells chased at 20°C for 24 h and the shifted to 37°C or 1 h; (lanes *13–15*) surface δ isolated from cells chased at 26°C for 24 h. Open arrowheads show the position of the δ subunit after Endoglycosidase H digestion.

dium butyrate for 24 h, and then shifted to 20°C for 40 h. Cells were permeabilized and labeled with different reagents to identify ER (anti-BiP mAb), Golgi (wheat germ agglutinin; WGA) and assembled AChR (mAb 35 or mAb 14). Cells were then labeled with the appropriate fluorescent-labeled antibody or WGA and visualized in a Zeiss IM35 microscope as described in Materials and Methods.

As discussed earlier (Fig. 2), mAb 35 is a conformation-specific antibody that preferentially binds assembled rather than unassembled α subunits (85–90% of assembled AChR, only 5.5% of unassembled α). To use this mAb as a marker of AChR complex in immunofluorescence microscopy studies, however, it is necessary to further determine what percentage of the total (assembled + unassembled) α which is recognized by mAb 35, is assembled AChR. A biochemical analysis of the cells was performed under conditions identical to those used for the immunofluorescence studies. When cells were labeled with [³⁵S]methionine for 30 h at 20°C, run on sucrose gradients, and immunoprecipitated with mAb 35, it was determined that 88–90% of the α polypeptide that was bound by this mAb, was assembled (data not shown). Thus, mAb 35 can be used as a marker for assembled AChR complex for our immunofluorescence studies. When mAb 35 is used to localize intracellular assembled AChR, a staining pattern characteristic of ER is obtained (Fig. 10 *A*). A comparison of this pattern with that obtained (Fig. 10 *E*) by staining All-11 cells with a marker for ER (an mAb to BiP or GRP78 [Bole et al., 1986], a resident protein of the ER [Hurtley and Helenius, 1989]) shows that the patterns are virtually identical. The cells shown in Fig. 10 *A* and *E* were also stained with a golgi-specific marker (fluorescein-conjugated WGA, shown in Fig. 10 *B* and *F*, respectively) and it can be seen that this pattern is clearly distinct from those obtained with mAbs to AChR or an ER protein. Another conformation-specific mAb (mAb 14) that recognizes as-

sembled α subunits but not SDS denatured (Tzartos and Lindstrom, 1980) or individually expressed α polypeptides (Loutrari, H., and T. Claudio, unpublished observations) was also used to localize AChR complexes in All-11 cells. The staining pattern obtained (Fig. 10 *C*) is identical to that of mAb 35. From these results, we conclude that the majority of intracellular AChR oligomers reside in the ER.

If AChR-expressing fibroblasts are shifted to 37 from 20°C, there is rapid transport of intracellular assembled AChR to the plasma membrane within 30 min. AChR-expressing All-11 cells treated for 30 min at 37°C and then labeled with mAb 35 are shown in Fig. 11 *A*. In these cells, the staining pattern of AChR is now reminiscent of Golgi staining (shown in *B* with fluorescein-conjugated WGA). Since *Torpedo* AChRs cannot assemble at 37°C, we are able to visualize the movement of preassembled AChRs (assembled at 20°C) to the cell surface via the Golgi apparatus.

The biochemical (acquisition of endoglycosidase H resistance) results indicated that AChR assembly occurred before the medial stack of the Golgi apparatus. The fluorescence microscopy results further localize this assembly to the ER. Assembled *Torpedo* AChRs can be "chased" to the cell surface with a temperature shift to 37°C. When this is done, AChRs can be detected in the Golgi apparatus for the first time. These results indicate that AChRs are sequestered within the ER and that once released, transport to the cell surface is rapid.

Effect of Forskolin on the Intracellular Distribution of Assembled AChR

Our endoglycosidase H and immunofluorescence microscopy results demonstrate that the majority of assembled AChRs reside in the ER and that the subsequent intracellular transport to the cell surface is rapid. We performed two sets of
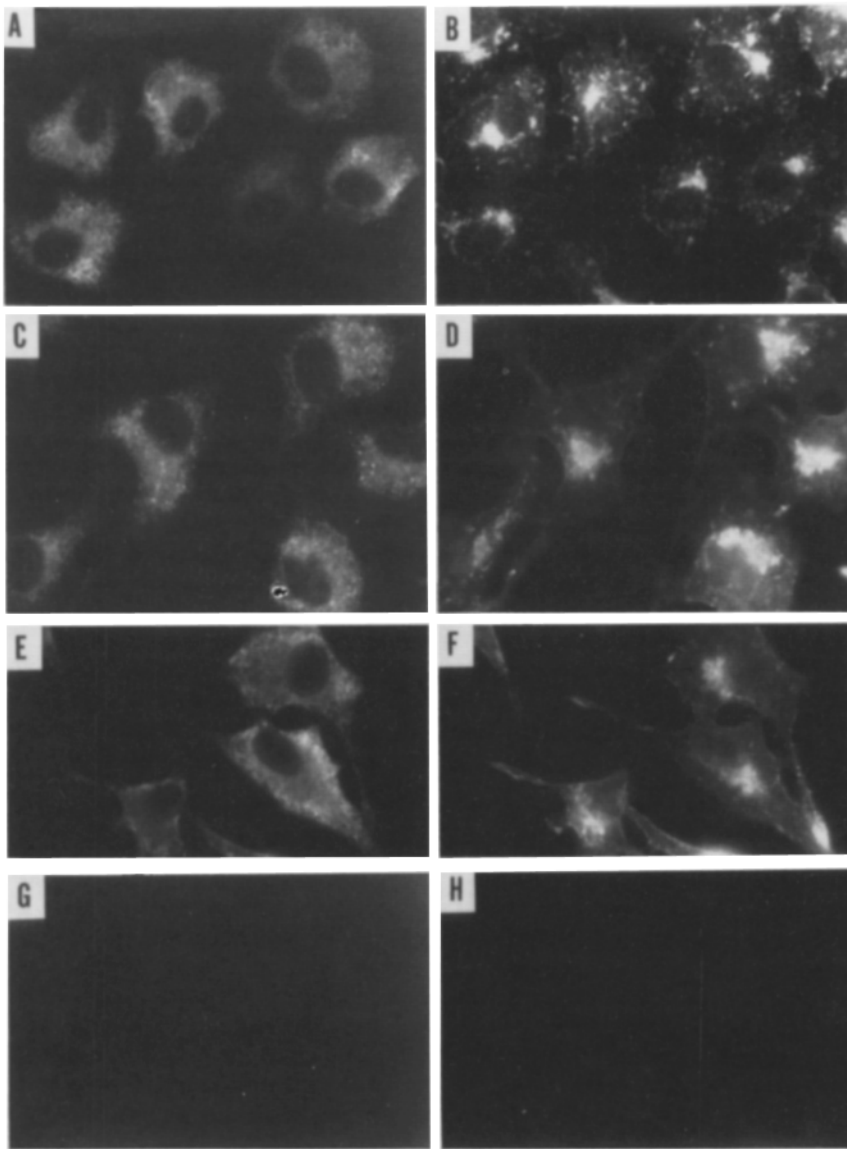
Figure 10. Immunofluorescent localization of intracellular AChR in All-11 cells. Fixed and permeabilized All-11 cells were first labeled in (*A*) with mAb 35 (anti-AChR mAb), in (*C*) with mAb 14 (anti-AChR mAb), in (*E*) with anti-BiP mAb (a resident protein of the ER), and then labeled with phycoerythrin-conjugated anti–rat IgG. These cells were double labeled with fluorescein-conjugated WGA (*B, D,* and *F*). No labeling was detected using rhodamine filters in the absence of primary antibody (*G*) or using fluorescein filters in the absence of fluorescein WGA. All-11 cells were incubated in sodium butyrate media at 37°C for 48 h, then shifted to 20°C for an additional 36 h before labeling.

experiments to determine if release from this compartment might be a site of regulation by forskolin. Cells were pulse labeled, chased with or without forskolin, and intracellular assembled subunits were monitored for endoglycosidase H sensitivity. As shown in Fig. 12, intracellular assembled AChRs in forskolin-treated cells (lane *3*) were completely endoglycosidase H sensitive as were intracellular assembled AChRs in nonforskolin-treated cells (lane 2), indicating that forskolin does not induce the release of AChRs from its site of assembly in the ER. This result was confirmed by im-
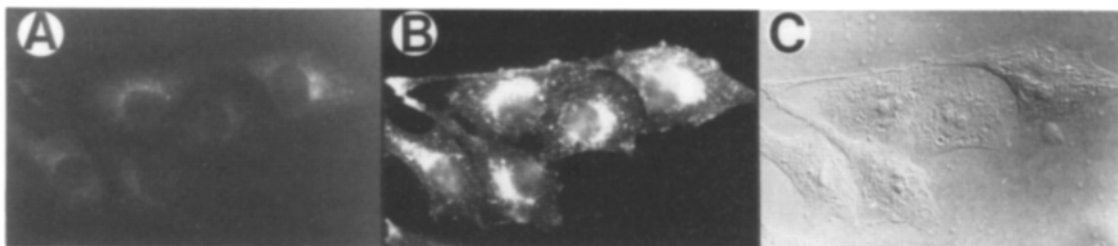

Figure 11. Localization of internal AChR in All-11 cells after temperature shift to 37°C. All-11 cells were temperature shifted from 37 to 20°C (see legend to Fig. 10) and then returned to 37°C for 30 min. Cells were labeled by mAb 35 indirect immunofluorescence (*A*) and fluorescein WGA (*B*). The differential interference contrast (D.I.C.; Zeiss) image of the cells is shown in (*C*).
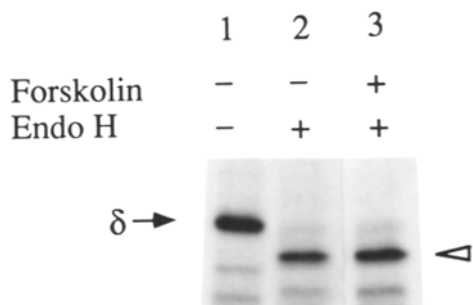
Figure 12. Endoglycosidase H sensitivity of the δ subunit in for-skolin-treated cells. All-11 cells were pulse labeled with 150 μCi/ml [^{35}S]methionine for 30 min at 37°C and then shifted to 20°C in the presence or absence of 100 μM forskolin for 24 h. Cells were lysed and assembled AChR oligomers were immunoprecipitated with mAb 35. The immunoprecipitated subunits were digested with en-doglycosidase H as described in Materials and Methods, and the digested subunits were reimmunoprecipitated with polyclonal anti-sera to the δ subunit, and then analyzed by SDS-PAGE. (Lane 1) mock-teated lysate showing the position of undigested, assembled δ subunit. (Lane 2) endoglycosidase H treatment of control lysates showing that assembled δ subunit is sensitive to this treatment. (Lane 3) endoglycosidase H treatment of forskolin-treated lysates showing that assembled δ subunit in these cells is similarly sensitive to this treatment (open arrowhead). It can be seen that the in-creased amounts of assembled subunits which were induced by for-skolin treatment, are in the endoglycosidase H–sensitive pool.

munofluorescence microscopy which showed that forskolin did not alter the intracellular distribution of AChR (compare forskolin treatment in Fig. 13 A with Fig. 10 A). Our conclusion from these experiments and those presented in Figs. 7 and 8, is that forskolin appears to act by increasing assembly efficiency, not by causing a shift in the intracellular distribution of assembled AChR.

Discussion

In this study we show that two independent treatments, lower temperature and increased intracellular cAMP, can increase AChR expression by increasing the efficiency of subunit as-sembly. The present results suggest two nonexclusive mecha-nisms by which assembly efficiency can be modulated. First, these treatments may decrease the degradation rate of the un-assembled subunits, thereby increasing the intersubunit in-teraction time and promoting oligomerization. Second, these treatments may induce conformational changes in the unas-sembled subunits which allow assembly to occur more read-ily. Assembled subunits are less sensitive to proteolysis which leads to an overall increase in AChR expression. Both mechanisms may account for both the temperature and the cAMP effect.

That impairment of subunit degradation accounts for some of the observed increased assembly efficiency is supported by several observations. It has been shown that assembled, cell surface AChRs in cultured muscle cells turnover more slowly at reduced temperatures (Devreotes and Fambrough, 1975). We find a similar decrease in turnover rate of Torpedo AChRs expressed in fibroblasts (∼14 h at 37°C, ∼60 h at 26°C; Claudio et al., 1989b). If we measure the lifetimes of the individual unassembled subunits, we observe values of 12–40 min at 37°C, 50–90 min at 28°C (Claudio et al., 1989a), 2–3 h at 26°C (Green et al., 1991), and 10–19 h at 20°C (data not shown). In addition, although assembly of mouse AChR subunits occurs at 37°C, this process was found to be more efficient at lower temperatures (Fig. 6 and Table II). These results are most consistent with the notion that cellular degradative enzymes are inhibited at lower tem-peratures, with the result that unassembled subunits are not degraded and are thus available for assembly. If this is true, why do we see assembly of mouse but not Torpedo subunits at 37°C?
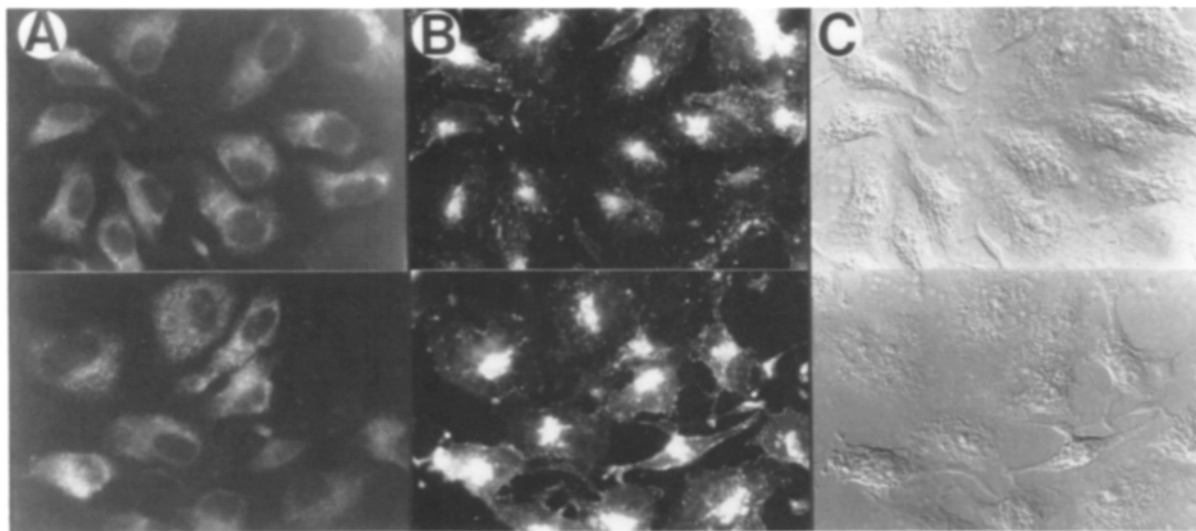

Figure 13. Immunofluorescent localization of AChR in forskolin-treated cells. Forskolin-treated All-11 cells were labeled by mAb 35 indirect immunofluorescence (A) and fluorescein WGA (B). All-11 cells were incubated in sodium butyrate-media for 36 h at 37°C and then in-cubated at 20°C for 36 h in this media supplemented with 100 μm forskolin. (C) D.I.C. image (Zeiss) of the cells.

Our results show that the rate of assembly of mouse AChR at 26 and 20°C is significantly faster than that of *Torpedo*. One possibility is that mouse subunits are able to assemble at 37°C before they are acted upon by cellular proteases, while *Torpedo* subunits largely degrade at this temperature before assembly occurs. The β subunit from *Torpedo* has a half-life of only ~12 min at 37°C, ~50 min at 28°C, ~3 h at 26°C, and ~13 h at 20°C. Since assembly of *Torpedo* subunits at 26°C is first detected after 2 h of chase (Fig. 3), it is likely that the majority of subunits are degraded before they assemble, thus accounting for the low assembly efficiency. The reason for the rapid degradation of *Torpedo* subunits at 37°C is likely because of misfolding of the polypeptides at nonpermissive temperatures (Paulson and Claudio, 1990). It has been shown with other temperature-sensitive synthesis mutants that misfolded polypeptides are rapidly degraded (Hurtley and Helenius, 1989) and thus it is a likely explanation for why *Torpedo* subunits are degraded so quickly at 37°C.

The possibility that assembly efficiency is increased because of conformational changes which allow assembly to occur more readily is supported by several observations. The acquisition of high affinity BuTx binding and mAb 35 binding to the α subunit are both thought to be measures of a requisite maturational step of this polypeptide before assembly of the subunit into an AChR complex can occur (Merlie and Lindstrom, 1983). We have shown previously that there is an increase in binding of both BuTx and mAb 35 to the α subunit as the temperature at which α-expressing cells are grown is changed from 37 to 26°C (Paulson and Claudio, 1990). If BuTx and mAb 35 binding are characteristics of mature subunits, then this shows that the α subunit assumes a more mature conformation when shifted to lower temperatures. If these maturational steps are necessary prerequisites for assembly, then the lower temperature more readily allows *Torpedo* subunits to undergo conformational changes necessary for assembly. The present results also address the nature of the conformational misfolding at 37°C. When misfolded, membrane proteins often form disulfide-linked homoaggregates (Machamer and Rose, 1988; Hurtley and Helenius, 1989). We have found that a small portion of the α subunits synthesized at 37°C are disulfide-linked aggregates of dimers, trimers, and larger complexes (Paulson, H. P., A. F. Ross, W. N. Green, and T. Claudio. In press), and that this proportion decreases when cells are shifted to 26°C. However, the majority of subunits synthesized at 37°C sediment from 6-13S as variably sized homoaggregates that are not covalently bound. Our present finding shows that the misfolding which occurs at higher temperatures is readily and completely reversed when subunits are shifted to a permissive temperature (Table I). This suggests that the misfolded subunits are noncovalently aggregated, since it is more likely that a noncovalent conformational change, rather than a covalent modification would be this readily reversible.

We have previously shown that the lifetime of all four subunits in All-11 cells is markedly extended when cells are treated with either forskolin or a cAMP analog (Green et al., 1991). In contrast to lower temperature, however, these agents do not impair cellular degradation mechanisms but rather appear to induce increased intersubunit interactions leading to increased assembly (Green et al., 1991). Since the lifetimes of individual subunits are significantly shorter than

assembled oligomers (Claudio et al., 1989*a*), it is likely that unassembled subunits are in protease-sensitive conformations, and that once assembled, subunits assume conformations which are less susceptible to degradation. Thus, the extended lifetimes seen when cells are treated with agents which increase intracellular cAMP result from an increase in assembly efficiency. How might cAMP influence subunit assembly? The best defined mechanism of action of cAMP is activation of a cellular protein kinase. This cAMP-dependent protein kinase is known to phosphorylate the γ and δ subunits of AChR (Huganir and Greengard, 1983). We have shown that the phosphorylation states of γ and δ subunits change as subunits move along the biosynthetic pathway, suggesting a role for phosphorylation in AChR biogenesis (Ross et al., 1987; Green, W. T., and T. Claudio, 1988. *Soc. Neurosci. Abstr.* 14:1045. (419.3). It is possible that cAMP phosphorylates a site(s) on the γ and/or δ subunit which promotes interactions with other subunits leading to a more efficient assembly process.

After subunit synthesis in the ER, the AChRs are transported to the Golgi apparatus (Fambrough and Devreotes, 1978) and then, via transport vesicles (Bursztajn and Fischbach, 1984), to the cell surface. While some studies have suggested that subunit assembly occurs in the Golgi apparatus (Fambrough and Devreotes, 1978; Merlie and Lindstrom, 1983; Ross et al., 1987), others have suggested that oligomerization precedes exit from the ER (Smith et al., 1987). In the present study we use two independent methods, acquisition of endoglycosidase H resistance and immunofluorescence microscopy, to identify the intracellular site of assembly. The finding that all detectable intracellular assembled δ subunits are endoglycosidase H sensitive shows that assembly precedes transport to the medial Golgi apparatus and that AChR oligomers pass quickly through the Golgi apparatus to the cell surface. Several observations indicate that this is not an artifact of the 20°C incubations. (*a*) A 20°C temperature block is only effective for a few hours, not 24 h as is used in our study. Although there is a partial temperature block of transport at 20°C, this block was shown to be at the *trans*-Golgi network (Saraste et al., 1986). If our 20°C incubations caused an artificial block of AChR transport in the *trans*-Golgi network, then the subunits would be endoglycosidase H resistant, not sensitive, as we find them. (*b*) The same results (no detectable intracellular assembled δ subunit with attached complex carbohydrates) were obtained when All-11 cells were incubated at 20 or 26°C (Fig. 7), yet no alteration of intracellular transport has been reported to occur at 26°C. Thus, these data all indicate that assembly is occurring before the medial stack of the Golgi apparatus. To further identify the site of assembly, immunofluorescent microscopic studies were performed. The results of these studies show that assembled AChR is located in the ER (Fig. 10). The only time localization in the Golgi can be observed is when cells are shifted to 37°C to induce a synchronous movement of AChRs to the plasma membrane. We are able to achieve this synchronous movement because *Torpedo* AChR subunits do not assemble at 37°C and once formed, *Torpedo* AChR complex is stable even when shifted to a temperature (37°C) that is not permissive for assembly (Paulson and Claudio, 1990).

Taken together, our results indicate that AChR oligomerization is not sufficient for transport out of the ER to the cell

surface. Oligomerization has been shown to be necessary, but not sufficient, for transport out of the ER for influenza hemagglutinin (Gething et al., 1986), class 1 MHC antigens (Miyazaki et al., 1986a,b), and VSV G proteins (Doms et al., 1988). It is possible that specific signals, the nature of which are unknown, are necessary for release of AChR oligomers from the ER. Although regulation of surface expression at the point of release from the ER has been reported to occur with other cell surface proteins, including the T cell receptor (Bonifacino et al., 1990), to date this has not been demonstrated for the AChR. A current goal of our laboratory concerns the mechanisms regulating the release of AChR oligomers from the ER.

References

Bole, D. G., L. M. Hendershot, and J. F. Kearney. 1986. Posttranslational association of immunoglobulin heavy chain binding protein with nascent heavy chains in nonsecreting and secreting hybridomas. *J. Cell Biol.* 102:1558–1566.

Bonifacino, J. S., S. A. McCarthy, J. E. Maguire, T. Nakayama, D. S. Singer, R. D. Klausner, and A. Singer. 1990. Novel post-translational regulation of TCR expression in CD4$^+$CD8$^+$ thymocytes influenced by CD4. *Nature (Lond).* 344:247–251.

Bursztajn, S., and G. D. Fischbach. 1984. Evidence that coated vesicles transport acetylcholine receptors to the surface of chick myotubes. *J. Cell Biol.* 98:498–506.

Claudio, T. 1989. Molecular genetics of acetylcholine receptor-channels. *In* Frontiers in Molecular Biology: Molecular Neurobiology Volume. D. M. Glover and B. D. Hames, editors. IRL Press, Oxford. 63–142.

Claudio, T., and M. A. Raftery. 1977. Immunological comparison of acetylcholine receptors and their subunits from species of electric ray. *Arch. Biochem. Biophys.* 181:484–489.

Claudio, T., W. N. Green, D. S. Hartman, D. Hayden, H. L. Paulson, F. J. Sigworth, S. M. Sine, and A. Swedlund. 1987. Genetic reconstitution of functional AChR channels in mouse fibroblasts. *Science (Wash. DC).* 238:1688–1694.

Claudio, T., H. L. Paulson, W. N. Green, D. Hartman, A. F. Ross, and D. Hayden. 1989a. Fibroblasts transfected with *Torpedo* acetylcholine receptor β, γ, and δ subunit cDNAs express functional AChRs when infected with a retroviral α-recombinant. *J. Cell Biol.* 108:2277–2290.

Claudio, T., D. S. Hartman, W. N. Green, A. F. Ross, and H. L. Paulson. 1989b. Stable expression of multisubunit protein complexes in mammalian cells. *In* NATO ASI Series H, Cell Biology, Molecular Biology of Neuroreceptors and Ion Channels. A. Maelicke, editor. Springer Verlag, Berlin, Vol. 32. 469–480.

Devreotes, P. N., and D. Fambrough. 1975. Acetylcholine receptor turnover in membranes of developing muscle fibers. *J. Cell Biol.* 65:335–358.

Doms, R. W., A Ruusala, C. Machamer, J. Helenius, A. Helenius, and J. K. Rose. 1988. Differential effects of mutations in three domains on folding, quaternary structure, and intracellular transport of vesicular stomatitis virus G protein. *J. Cell Biol.* 107:89–99.

Fambrough, D. M., and P. N. Devreotes. 1978. Newly synthesized acetylcholine receptors are located in the Golgi apparatus. *J. Cell Biol.* 76:237–244.

Fontaine, B., A. Klarsfeld, and J. P. Changeux. 1987. Calcitonin gene-related peptide and muscle activity regulate acetylcholine receptor α-subunit mRNA levels by distinct intracellular pathways. *J. Cell Biol.* 105:1337–1342.

Gething, M.-J., K. McCammon, and J. Sambrook. 1986. Expression of wild-type and mutant forms of influenza virus hemagglutinin: the role of folding in intracellular transport. *Cell.* 46:939–950.

Goldman, D., J. Boulter, S. Heinemann, and J. Patrick. 1985. Muscle denervation increases the levels of two mRNAs coding for the acetylcholine receptor α subunit. *J. Neurosci.* 5:2553–2558.

Goldman, D., H. R. Brenner, and S. Heinemann. 1988. Acetylcholine receptor α-, β-, γ-, and δ-subunit RNA levels are regulated by muscle activity. *Neuron.* 1:329–333.

Green, W. N., A. F. Ross, and T. Claudio. 1991. cAMP stimulation of acetylcholine receptor expression is mediated through posttranslational mechanisms. *Proc. Natl. Acad. Sci. USA.* 88:854–858.

Gu, Y., E. Ralston, C. Murphy-Erdosh, and Z. W. Hall. 1989. Acetylcholine receptor in a C2 muscle cell variant is retained in the endoplasmic reticulum. *J. Cell Biol.* 109:729–738.

Harris, D. A., D. L. Falls, R. M. Dill-Devor, and G. D. Fischbach. 1988. Acetylcholine receptor-inducing factor from chicken brains increases the level of mRNA encoding the receptor α subunit. *Proc. Natl. Acad. Sci. USA.* 85:1983–1987.

Horovitz, O., D. Knaack, T. R. Podleski, and M. M. Salpeter. 1989. Acetylcholine receptor α-subunit mRNA is increased by ascorbic acid in cloned L5 muscle cells: northern blot analysis and in situ hybridization. *J. Cell Biol.* 108:1823–1832.

Huganir, R. L., and P. Greengard. 1983. cAMP-dependent protein kinase phosphorylates the nicotinic acetylcholine receptor. *Proc. Natl. Acad. Sci. USA.* 80:1130–1134.

Hurtley, S. M., and A. Helenius. 1989. Protein oligomerization in the endoplasmic reticulum. *Annu. Rev. Cell Biol.* 5:277–307.

Klarsfeld, A., and J. P. Changeux. 1985. Activity regulates the levels of acetylcholine receptor α-subunit mRNA in cultured chicken myotubes. *Proc. Natl. Acad. Sci. USA.* 82:4558–4562.

Laemmli, U. K. 1970. Cleavage of structural proteins during the assembly of the head of bacteriophage T4. *Nature (Lond.).* 227:680–685.

Machamer, C. E., and J. K. Rose. 1988. Vesicular stomatitis virus G proteins with altered glycosylation sites display temperature-sensitive intracellular transport and are subject to aberrant intermolecular disulfide bonding. *J. Biol. Chem.* 263:5955–5960.

Merlie, J. P., and J. Lindstrom. 1983. Assembly in vivo of mouse muscle acetylcholine receptor: identification of an α subunit species that may be an assembly intermediate. *Cell.* 34:747–757.

Miyazaki, J.-I., E. Appella, and K. Ozato. 1986a. Intracellular transport blockade caused by disruption of the disulfide bridge in the third external domain of major histocompatibility class 1 antigen. *Proc. Natl. Acad. Sci. USA.* 83:757–761.

Miyazaki, J.-I., E. Appella, H. Zhao, J. Forman, and K. Ozato. 1986b. Expression and function of a nonglycosylated major histocompatibility class 1 antigen. *J. Exp. Med.* 163:856–871.

Nomoto, H., N. Takahashi, Y. Nagaki, S. Endo, Y. Arata, and K. Hayashi. 1986. Carbohydrate structures of acetylcholine receptor from *Torpedo californica* and distribution of oligosaccharides among the subunits. *Eur. J. Biochem.* 157:233–244.

Paulson, H. P., and T. Claudio. 1990. Temperature-sensitive expression of all-*Torpedo* and *Torpedo*-rat hybrid AChR in mammalian muscle cells. *J. Cell Biol.* 110:1705–1717.

Paulson, H. P., A. F. Ross, W. N. Green, and T. Claudio. 1991. Analysis of early events in acetylcholine receptor assembly. *J. Cell Biol.* In press.

Popot, J.-L., and P.-J. Changeux. 1984. Nicotinic receptor of acetylcholine: structure of an oligomeric integral membrane protein. *Physiol. Rev.* 64:1162–1239.

Ross, A. F., M. Rapuano, J. H. Schmidt, and J. M. Prives. 1987. Phosphorylation and assembly of nicotinic acetylcholine receptor subunits in cultured chick muscle cells. *J. Biol. Chem.* 262:14640–14647.

Roth, J. 1987. Subcellular organization of glycosylation in mammalian cells. *Biochim. Biophys. Acta.* 906:405–436.

Salpeter, M. M. 1987. Development and neural control of the neuromuscular junction and of the junctional acetylcholine receptor. *In* Neurology and Neurobiology. Volume 23. M. M. Salpeter, editor. Alan R. Liss Inc., New York. 55–115.

Saraste, J., G. E. Palade, and M. G. Farquhar. 1986. Temperature-sensitive steps in the transport of secretory proteins through the Golgi complex in exocrine pancreatic cells. *Proc. Natl. Acad. Sci. USA.* 83:6425–6429.

Shieh, B. H., M. Ballivet, and J. Schmidt. 1987. Quantitation of an alpha subunit splicing intermediate: evidence for transcriptional activation in the control of acetylcholine receptor expression in denervated chick skeletal muscle. *J. Cell Biol.* 104:1337–1341.

Smith, M. M., J. Lindstrom, and J. P. Merlie. 1987. Formation of the α-bungarotoxin binding site and assembly of the nicotinic acetylcholine receptor subunits occur in the endoplasmic reticulum. *J. Biol. Chem.* 262:4367–4376.

Takami, K., Y. Kawai, S. Shiosaka, Y. Lee, S. Girgis, C. J. Hillyard, I. MacIntyre, P. C. Emson, and M. Tohyama. 1985. Immunohistochemical evidence for the coexistence of calcitonin gene-reglated peptide- and choline acetyltransferase-like immunoreactivity in neurons of the rat hypoglossal, facial and ambiguous nuclei. *Brain Res.* 328:386–389.

Tsay, H.-J., and J. Schmidt. 1989. Skeletal muscle denervation activates acetylcholine receptor genes. *J. Cell Biol.* 108:1523–1526.

Tzartos, S. J., and J. M. Lindstrom. 1980. Monoclonal antibodies used to probe acetylcholine receptor structure: localization of the main immunogenic region and detection of similarities between subunits. *Proc. Natl. Acad. Sci. USA.* 77:755–759.